New phases of $SU(3)$ and $SU(4)$ at finite temperature

Joyce C. Myers* and Michael C. Ogilvie+

Department of Physics, Washington University, St. Louis, Missouri 63130, USA

(Received 13 October 2007; published 25 June 2008)

The addition of an adjoint Polyakov loop term to the action of a pure gauge theory at finite temperature leads to new phases of $SU(N)$ gauge theories. For $SU(3)$, a new phase is found which breaks $Z(3)$ symmetry in a novel way; for $SU(4)$, the new phase exhibits spontaneous symmetry breaking of $Z(4)$ to $Z(2)$, representing a partially-confined phase in which quarks are confined, but diquarks are not. The overall phase structure and thermodynamics is consistent with a theoretical model of the effective potential for the Polyakov loop based on perturbation theory.

DOI: 10.1103/PhysRevD.77.125030 PACS numbers: 12.38.Gc, 11.10.Wx, 11.15.Ha

I. INTRODUCTION

It is well established that $SU(N)$ gauge theories in $3+1$ dimensions have a low-temperature phase in which quarks are confined, and a high-temperature phase where quarks are deconfined, often referred to as the quark-gluon plasma phase. The deconfinement phase transition in pure gauge theories, i.e., without quarks, is understood theoretically as a transition between a low-temperature phase where a global $Z(N)$ symmetry is unbroken to a high-temperature phase where $Z(N)$ symmetry is spontaneously broken [1]. Simulations indicate that the transition from confined phase to deconfined phase is similar for all $N \geq 3$. The global $Z(N)$ symmetry appears to always break completely, with no residual unbroken subgroup.

The addition of a term of the form

$$-\int d^3x h_A \,\mathrm{Tr}_A P(\vec{x}) = -T\int_0^\beta dt \int d^3x h_A \,\mathrm{Tr}_A P(\vec{x}) \quad (1)$$

to the Euclidean action of pure $SU(N)$ gauge theories at finite temperature leads to new phases with novel properties. Here $P(\vec{x})$ is the Polyakov loop at the spatial point $\vec{x}$, given by the usual path-ordered exponential of the temporal component of the gauge field A_0 in the Euclidean time direction. The temporal origin of P is irrelevant due to the trace; because the trace is in the adjoint representation, this additional term respects $Z(N)$ symmetry. Of course, this additional term in the action is neither local nor renormalizable in $3+1$ dimensions. Thus we must regard this model as an effective theory defined at fixed lattice spacing or by some other cutoff. There will be a finite renormalization of the parameter h_A in comparing lattice results with continuum.

This additional term directly changes the effective potential. For a pure $SU(N)$ gauge theory, the effective potential V_{eff} can be written as a character expansion of the form

$$V_{\mathrm{eff}} = \sum v_R \,\mathrm{Tr}_R P \quad (2)$$

where the sum is over all representations of zero N-ality, i.e., invariant under $Z(N)$. Terms of this form can be induced at one loop by certain topological excitations [2–4] as well as by particles in the adjoint representation. A one-loop calculation shows that the contribution to the effective potential of a heavy particle of mass M in the adjoint representation, either boson or fermion can be approximated in $3+1$ dimensions as

$$-\left[\frac{(2s+1)M^2T^2}{\pi^2}K_2(M/T)\right]\mathrm{Tr}_A(P) = -Th_A\,\mathrm{Tr}_A(P) \quad (3)$$

where T is the temperature and $2s+1$ accounts for spin [5]. The parameter h_A is positive in this case. The effect of such particles can be included at lowest order in h_A in the effective potential by the shift $v_A \to v_A - Th_A$. A positive value of h_A favors the $Z(N)$-breaking deconfined phase. However, a term with h_A negative favors minimization of $\mathrm{Tr}_A P$. Because $\mathrm{Tr}_A P = |\mathrm{Tr}_F P|^2 - 1$, the minimization $\mathrm{Tr}_A P$ implies $\mathrm{Tr}_F P = 0$, a defining property of the confined phase. It is reasonable to expect that a sufficiently negative value of h_A might lead to a restoration of confinement at temperatures above the deconfinement temperature.

We were motivated to look for this symmetry restoration by recent theoretical work on various aspects of the Polyakov loop effective potential. In certain supersymmetric gauge theories on $R^3 \times S^1$, Davies *et al.* [2,3] have shown that finite-temperature monopoles give rise to a Polyakov loop effective potential that has a $Z(N)$-symmetric minimum for all values of the S^1 circumference, and is therefore in a confined phase. These models do not precisely represent systems at finite temperature, because the supersymmetric partners of the gauge fields obey periodic boundary conditions. Comparable calculations in nonsupersymmetric $SU(N)$ gauge theories at finite temperature are much more difficult. In $SU(2)$ gauge the-

*jcmyers@wustl.edu
+mco@wuphys.wustl.edu

ory, Diakonov *et al.* [4] have calculated the contribution to $V_{\rm eff}$ of finite-temperature instantons with nontrivial holonomy; such instantons have a color magnetic monopole content. Their work indicates an instability of the deconfined phase at sufficiently low temperature. In both of these examples, topological excitations give rise to a term in the effective potential corresponding to h_A negative.

A positive value of h_A decreases the deconfinement temperature. For negative values of h_A, we have found new phases for both $SU(3)$ and $SU(4)$. In the case of $SU(3)$, the new phase breaks $Z(3)$ symmetry in an unfamiliar way, characterized by a negative value for the Polyakov loop in the fundamental representation $\langle \mathrm{Tr}_F P\rangle < 0$. In the case of $SU(4)$, the global $Z(4)$ symmetry is spontaneously broken to $Z(2)$. The residual $Z(2)$ symmetry ensures that for the fundamental representation $\langle \mathrm{Tr}_F P\rangle = 0$, but $\langle \mathrm{Tr}_R P\rangle \neq 0$ for representations R that transform trivially under $Z(2)$, such as the **6** and the **10**.

II. SIMULATION RESULTS FOR $SU(3)$

The lattice action we have studied for $SU(3)$ and $SU(4)$ is

$$S = S_W + \sum_{\vec{x}} H_A \,\mathrm{Tr}_A P(\vec{x}) \tag{4}$$

where S_W is the Wilson action, defined conventionally as the sum over plaquettes. The sum in the second term is over all spatial sites, and naively $H_A = h_A a^3$. Most of our simulations were performed on $24^3 \times 4$ lattices, on a range of Wilson action β values ranging from 5.7 to 6.8. Although we motivate the additional parameter H_A as arising from heavy adjoint fermions, there is no renormalization of the gauge coupling as there would be with dynamical fermions. Thus the lattice spacing in physical units will be similar to that of the pure gauge theory. At $\beta = 6.5$, this leads to a spatial lattice size slightly larger than a fermi. This would be dangerously small for simulations with light dynamical quarks. However, the size is adequate here, because the deconfinement temperature of the pure gauge theory is higher than, for example, the chiral transition temperature for light fundamental quarks. We have checked our results on a larger lattice of size $32^3 \times 4$ with a smaller number of configurations, and have obtained results similar to those discussed below. The phase structure seen for $N_t = 4$ was also observed in simulations with $N_t = 2$ and 6.

The programs used for these simulation were developed using the programming framework FermiQCD [6]. Because the augmented lattice action S depends quadratically on the timelike link variable U_0 via the adjoint representation, the efficient heatbath methods developed for the standard lattice action cannot be used. We have used instead a recently developed $SU(N)$ over-relaxation algorithm [7] combined with the Metropolis algorithm. The over-relaxation algorithm, which operates on the full $SU(N)$ group rather than subgroups, proved to be fast and effective. Other algorithms which have been developed for fundamental plus adjoint actions could also be used [8,9]. A typical simulation on a $24^3 \times 4$ lattice consisted of 10 000 equilibration sweeps followed by 60 000 sweeps during which 2000 measurements were performed.

The approximate phase diagram for $SU(3)$ is shown in Fig. 1 for $N_t = 4$. The order parameter is $\mathrm{Tr}_F P$, where phases related by a global $Z(3)$ rotation are equivalent. It is convenient to project the order parameter onto the real axis. There are three distinct phases: a deconfined phase where the projected expectation value satisfies $\langle \mathrm{Tr}_F P\rangle > 0$, a confined phase where $\langle \mathrm{Tr}_F P\rangle = 0$, and an intermediate phase with $\langle \mathrm{Tr}_F P\rangle < 0$, which we refer to as the skewed phase. The standard practice for projecting the configuration-averaged value of $\mathrm{Tr}_F P$ onto the real axis by maximizing $\Re[z\mathrm{Tr}_F P]$ over all $z \in Z(N)$ must be slightly modified due to the presence of the skewed phase. The correct procedure is to find the $z \in Z(N)$ that maximizes $|\Re[z\mathrm{Tr}_F P]|$, and then use $\Re[z\mathrm{Tr}_F P]$ with that value of z as the projected order parameter. Without this additional step, configurations in the skewed phase are incorrectly assigned to the deconfined phase. In addition to the order parameter itself, generalized susceptibilities associated with the Polyakov loop in several representations were also obtained. The adjoint susceptibility arises naturally as the second derivative of the free energy with respect to h_A, and was the least noisy of the susceptibilities. The locations of the phase transitions were determined from the behavior of the order parameter and the peaks of the adjoint Polyakov loop susceptibility, checked against the

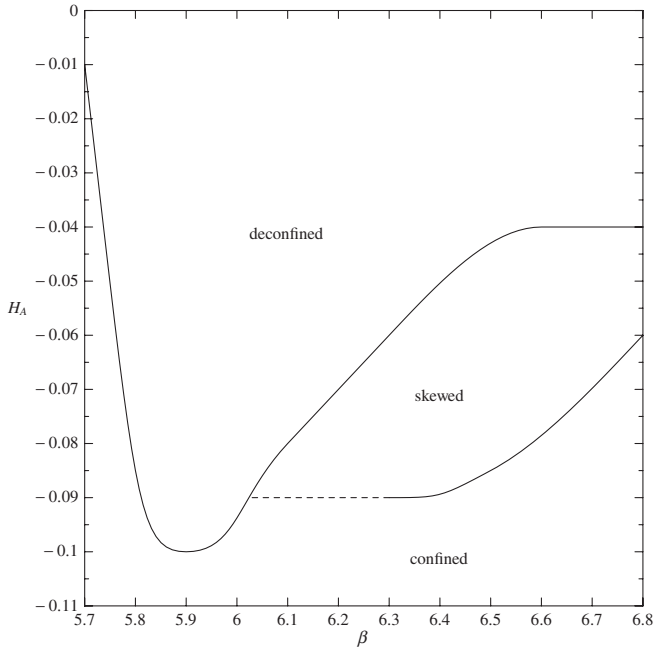

FIG. 1. $SU(3)$ phase diagram in the $\beta - H_A$ plane. The dotted line represents a simple extrapolation.

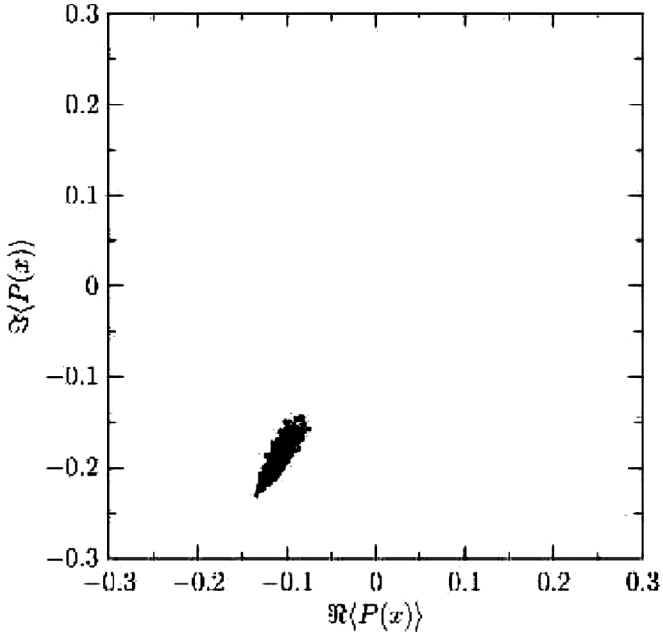

FIG. 2. $SU(3)$ Polyakov loop histogram at $\beta = 6.5$, $H_A = -0.05$.

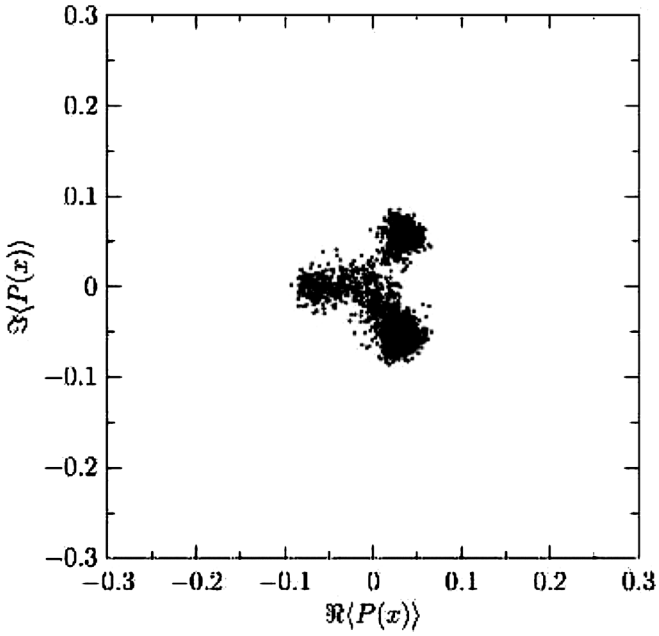

FIG. 4. $SU(3)$ Polyakov loop histogram at $\beta = 6.5$, $H_A = -0.08$.

histograms of the fundamental Polyakov loop. The dashed line in the phase diagram is an extrapolation. The phase transition between the skewed and confined phases is very difficult to resolve in this region, because the discontinuity in the order parameters becomes very small. We will use the notation H_{c1} for the values of H_A on the boundary between the deconfined and skewed phases, and H_{c2} for the boundary between the skewed and confined phases.

Figures 2–6 show histograms of the order parameter $\langle \mathrm{Tr}_F P\rangle$ for various values of H_A at $\beta = 6.5$. At $H_A = -0.06$, there is clear evidence for the new intermediate phase where $\langle \mathrm{Tr}_F P\rangle < 0$. The skewed phase breaks $Z(3)$ symmetry, as shown clearly by the histogram at $H_A = -0.08$, where all three possible skewed phases appear. The appearance of significant tunneling between the three phases on a $24^3 \times 4$ lattice is an indication that the tran-

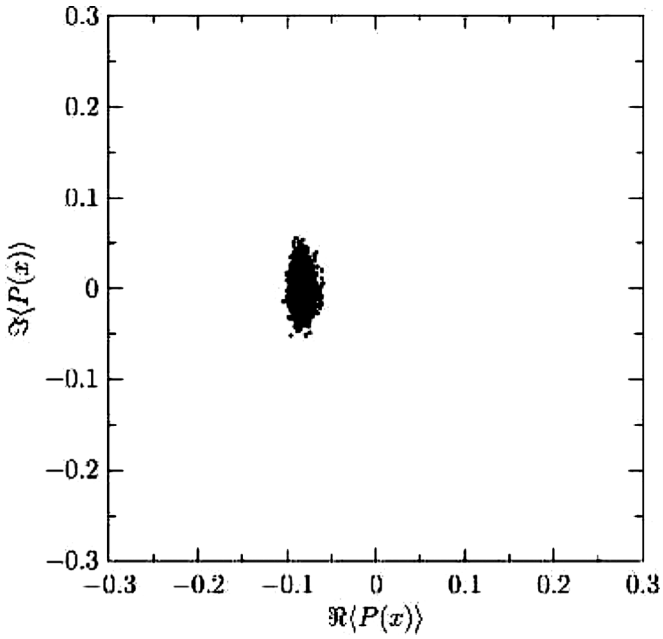

FIG. 3. $SU(3)$ Polyakov loop histogram at $\beta = 6.5$, $H_A = -0.06$.

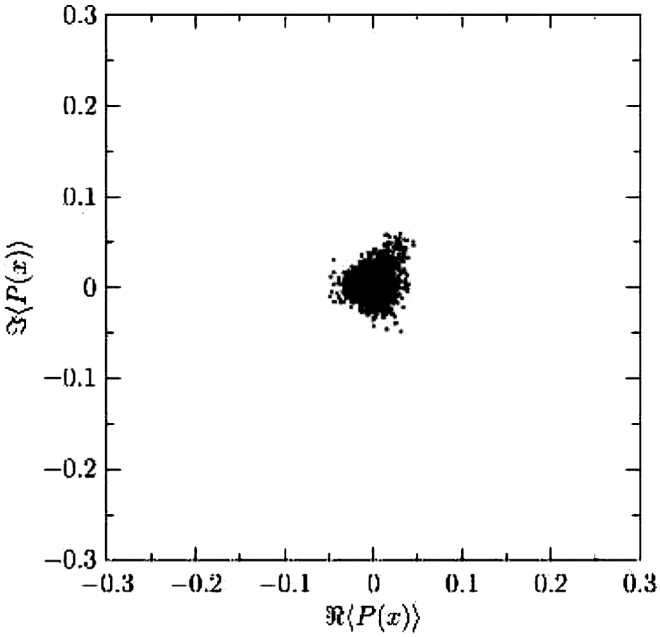

FIG. 5. $SU(3)$ Polyakov loop histogram at $\beta = 6.5$, $H_A = -0.1$.

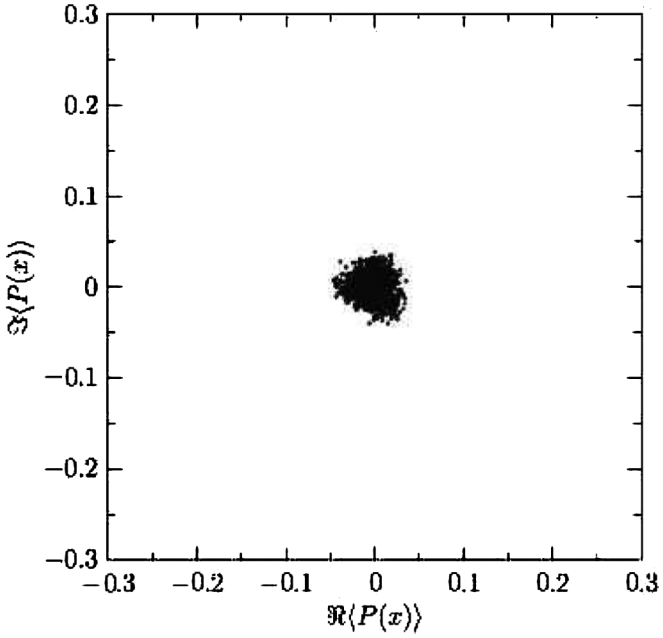

FIG. 6. $SU(3)$ Polyakov loop histogram at $\beta = 6.5$, $H_A = -0.11$.

sition from the skewed phase to the confined phase is very weak. The skewed phase differs from the deconfined phase not only in the orientation of the histograms, but also in the smaller magnitude of $\langle \mathrm{Tr}_F P \rangle$ for the skewed phase. Near H_{c1}, the orientation of fluctuations in histograms of the skewed phase is predominantly tangential, but becomes more radial as H_{c2} is approached. The transition between the deconfined and skewed phase is clearly first

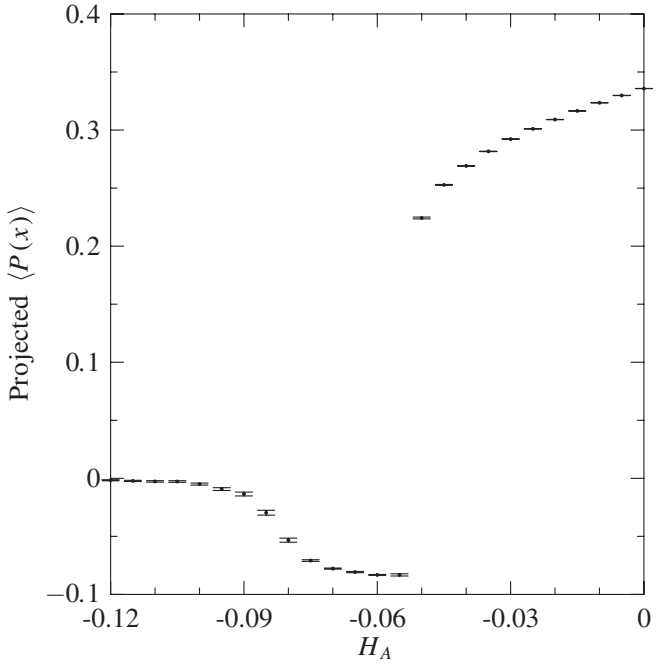

FIG. 7. Projected $\mathrm{Tr}_F P$ for $\beta = 6.5$.

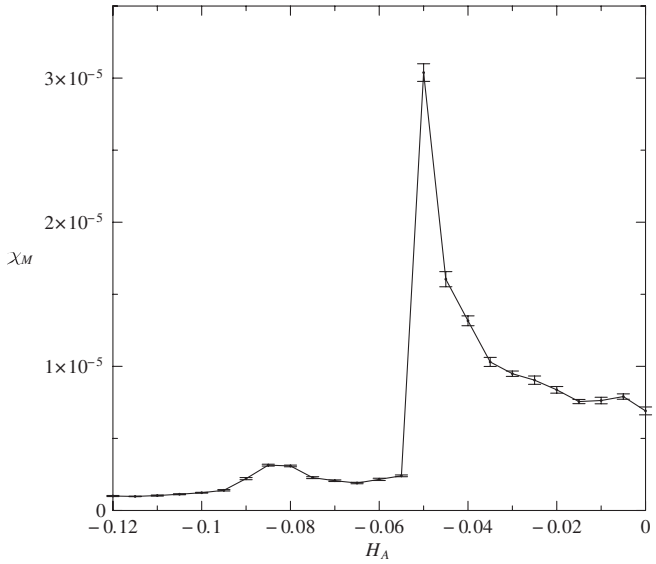

FIG. 8. Adjoint susceptibility χ_M for $\beta = 6.5$.

order because the order parameter shows a marked jump when changing sign. The transition between the skewed phase and the confined phase is likely to be first order, because it is associated with the universality class of the three-dimensional Potts model and its generalizations via Svetitsky-Yaffe universality. However, in simulations $\langle \mathrm{Tr}_F P \rangle$ shows a very small change at the skewed-confined transition, particularly near the apparent tricritical point. Empirically, for a given value of N_t, the skewed phase shows up clearly only for $N_s/N_t \geq 6$. On a $12^3 \times 6$ lattice, for example, the skewed phase always appears to coexist with either the deconfined phase or the confined phase. A detailed finite-size scaling analysis on very large lattices would be required to resolve the order of this transition with confidence.

Figure 7 shows the projected value of $\langle \mathrm{Tr}_F P \rangle$ for various values of H_A at $\beta = 6.5$. The presence of three distinct phases is clear. Note that the transition between the skewed and deconfined phases is much more abrupt than the transition between the skewed and confined phases. The adjoint susceptibility χ_M for $\beta = 6.5$ is shown in Fig. 8. There is a clear peak between the deconfined and skewed phases, and a much smaller peak separating the skewed and confined phases.

III. THEORY FOR $SU(3)$

A simple theoretical approach based on the effective potential V_{eff} for Polyakov loop eigenvalues reproduces the phase structure observed in simulations for $SU(3)$ and $SU(4)$. The effective potential has two parts. The first part is the one-loop expression for the free energy of gluons moving in a nontrivial, constant Polyakov loop background. The one-loop free energy density was first evaluated by Gross, Pisarski, and Yaffe [10], and by Weiss [11].

It is convenient to work in a gauge where A_0 is a constant element of the $SU(N)$ Lie algebra so that the background Polyakov loop is given simply by $P = \exp(i\beta A_0)$. The second contribution to the effective potential in our model is simply the term $-h_A T \mathrm{Tr}_A P$ that we have added to the gauge Lagrangian. At temperature T, our expression for V_{eff} is given by

$$V_{\mathrm{eff}} = -2\frac{1}{2}\mathrm{Tr}_A \int \frac{d^3k}{(2\pi)^3} T\sum_n \ln[(\omega_n - A_0)^2 + k^2] - h_A T \mathrm{Tr}_A P \quad (5)$$

where the sum is over Matsubara frequencies $\omega_n = 2\pi nT$. A useful form is

$$V_{\mathrm{eff}} = \sum_{j,k=1}^{N}\left(1 - \frac{\delta_{jk}}{N}\right)\left[-\frac{\pi^2 T^4}{45} + \frac{T^4}{24\pi^2}|\Delta\theta_{jk}|^2(2\pi - |\Delta\theta_{jk}|)^2\right] - h_A T\left(\left|\sum_{j=1}^{N} e^{i\theta_j}\right|^2 - 1\right) \quad (6)$$

where the angles θ_j are the eigenvalues of βA_0 and $|\Delta\theta_{jk}|$ is $|\theta_j - \theta_k| \mathrm{mod} 2\pi$. Thus V_{eff} is the sum of a one-loop term plus another term treated classically.

The phase diagram is found by minimizing V_{eff} as a function of the Polyakov loop eigenvalues. The two terms that make up V_{eff} have identical local extrema, and the problem of minimizing V_{eff} can be reduced to finding the minimum over this set. In the case of $SU(3)$, it is sufficient to consider V_{eff} as $\mathrm{Tr}_F P$ varies along the real axis. In this case, the eigenvalues of P may be taken to be the set $\{1, \exp(i\phi), \exp(-i\phi)\}$, and $\mathrm{Tr}_F P$ may be written as $1 + 2\cos(\phi)$. The effective potential is given by

$$V_{\mathrm{eff}}(\phi, T, h_A) = \frac{T^4}{6\pi^2}(8\phi^2(\phi - \pi)^2 + \phi^2(\phi - 2\pi)^2) - h_A T((1 + 2\cos(\phi))^2 - 1). \quad (7)$$

The extrema of V_{eff} occur at $\phi = 0$, $\phi = 2\pi/3$, and $\phi = \pi$. The values of $\mathrm{Tr}_F P$ for these values of ϕ are 3, 0, and -1, and we identify them with the deconfined, confined, and skewed phases, respectively. The set of eigenvalues $\{1, \exp(2\pi i/3), \exp(-2\pi i/3)\}$ is the unique set invariant under global $Z(3)$ transformations [12,13].

It is clear that the phase structure depends only on the dimensionless variable h_A/T^3. As h_A is lowered from zero, there is a first-order transition from the deconfined phase to the skewed phase. Setting the effective potential at $\phi = 0$ and $\phi = \pi$ equal, we find that the transition from the deconfined phase to the skewed phase takes place at $h_{c1}/T^3 = -\pi^2/48 \simeq -0.206$. As h_A decreases, another first-order transition, this time between the skewed and confined phases, occurs at $h_{c2}/T^3 = -5\pi^2/162 \simeq -0.305$. We plot the potential as a function of $\mathrm{Tr}_F P$ for values in the three phase in Figs. 9–11, corresponding to $H_A/T^3 = 0, -0.24, -0.35$.

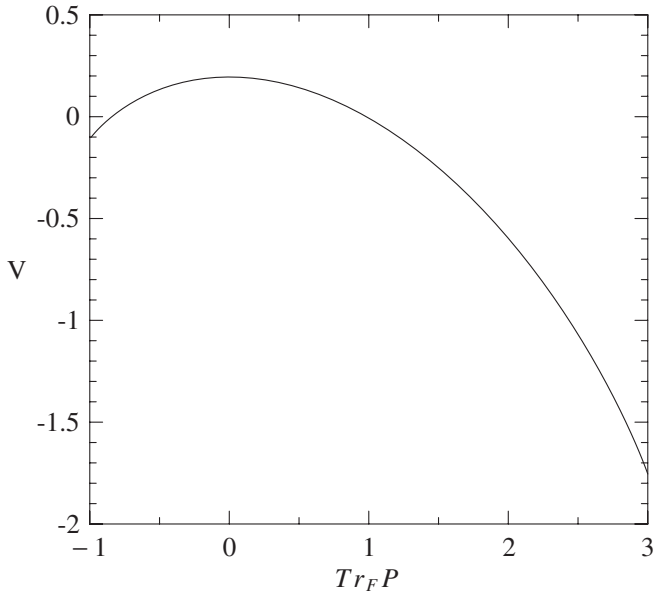

FIG. 9. Effective potential versus $\mathrm{Tr}_F P$ for the deconfined phase at $h_A/T^3 = 0$.

We cannot directly relate h_A and the corresponding lattice parameter H_A, because there is an unknown multiplicative renormalization relating the two. However, the ratio h_{c2}/h_{c1} is approximately 1.48. If we assume that the relation of h to H is approximately independent of h, we can compare with the results obtained from simulation. As shown in Fig. 1, the ratios H_{c2}/H_{c1} obtained vary from 1.27 at $\beta = 6.2$ to 1.44 at $\beta = 6.8$, with a maximum value of 1.73 in between.

As noted previously, our simulations show a pronounced asymmetry in the skewed phase between the fluctuations of

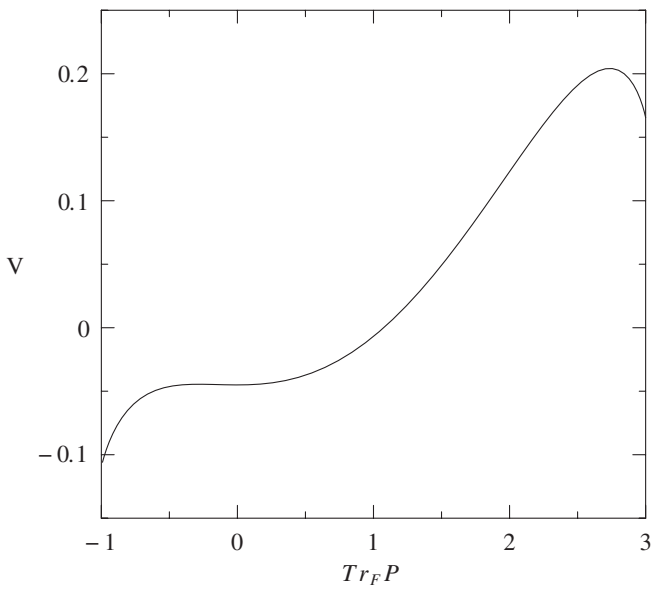

FIG. 10. Effective potential versus $\mathrm{Tr}_F P$ for the skewed phase at $h_A/T^3 = -0.24$.

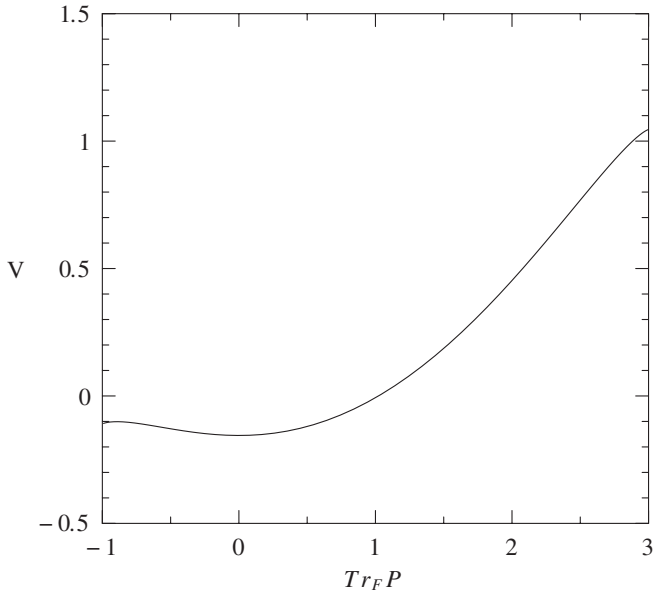

FIG. 11. Effective potential versus $\mathrm{Tr}_F P$ for the confined phase at $h_A/T^3 = -0.35$.

the imaginary and the real parts of $\mathrm{Tr}_F P$. Fluctuations in the projected imaginary part are associated with motion in the λ_8 direction, while fluctuations in the projected real part are due to motion in both the λ_8 and λ_3 directions. It is thus interesting that in the skewed phase, theory predicts an asymmetry in the screening masses obtained from small fluctuations in the eigenvalues of P. This is quite different from the behavior in the confined and deconfined phases, where theory predicts no asymmetry. We have

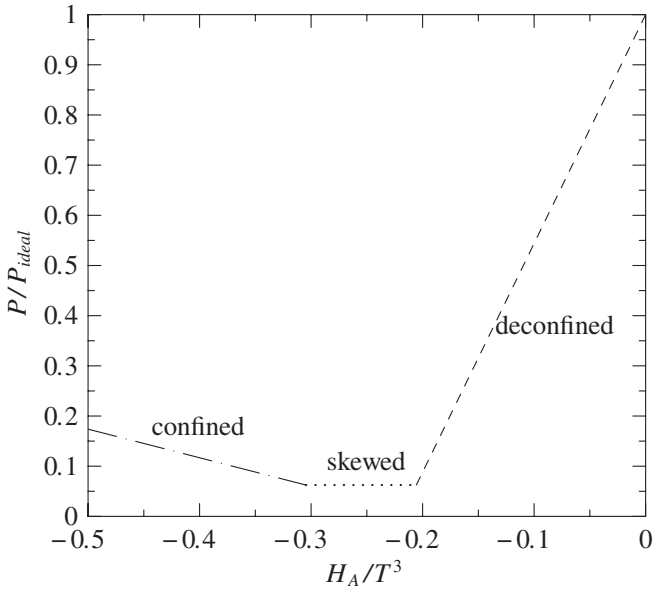

FIG. 12. Theoretical prediction for pressure normalized to black body pressure as a function of h_A.

$$\frac{m_3}{m_8} = \sqrt{\frac{1 + 2h_A/T^3}{-1 - 6h_A/T^3}}. \tag{8}$$

This ratio varies from 1.59 at h_{c1} to 0.69 at h_{c2}. This is on the order of the variation seen in the fluctuations of the real and imaginary parts of $\mathrm{Tr}_F P$, and probably accounts for the behavior seen in the histograms. This prediction for the mass ratio can be checked more directly in simulations by comparing the masses obtained from the correlation functions of the real and imaginary parts of the projected Polyakov loop in the skewed phase.

The pressure can be calculated from simulations along a path of constant β, using

$$\frac{p_2}{T^4} - \frac{p_1}{T^4} = N_t^3 \int_1^2 dH_A \langle \mathrm{Tr}_A P \rangle. \tag{9}$$

A detailed comparison of the pressure for all values of h_A would require knowledge of the relation between h_A and H_A. However, it is relatively simple to compare the change in the pressure from $h_A = H_A = 0$ to the deconfined-skewed phase boundary as well as the change in pressure across the skewed phase. Using V_{eff}, we find that the predicted change in p/T^4 from h_{c1} to 0 is $\pi^2/6 \simeq 1.64$; from h_{c2} to h_{c1} the net change is 0, as shown by Fig. 12. For comparison, the corresponding results from simulations at $\beta = 6.5$ are 1.64 ± 0.03 and -0.18 ± 0.07. In each case, the error is completely dominated by systematic error due to uncertainty in the location of the critical values of H_A, with statistical error at least an order of magnitude smaller.

IV. SIMULATION RESULTS FOR $SU(4)$

We have also simulated $SU(4)$ lattice gauge theories, again primarily on $24^3 \times 4$ lattices. As in the case of $SU(3)$, we find a new phase in the region $h_A < 0$, but the nature of the new phase is completely different. In this new, partially-confined phase, global $Z(4)$ symmetry is spontaneously broken to $Z(2)$. In this phase, particles in the fundamental representation (''$SU(4)$ quarks'') are still confined, but bound states of two such particles (''$SU(4)$ diquarks'') are not. Each irreducible representation of $SU(N)$ has an N-ality: if $z \in Z(N)$, $P \rightarrow zP$ induces a change $\mathrm{Tr}_R P \rightarrow z^k \mathrm{Tr}_R P$, where k is the N-ality of the representation R. The characteristic feature of the partially-confined phase in $SU(4)$ is that the expected value of Polyakov loops in $k = 1$ representations is zero, but not in $k = 2$ representations such as the **6** and the **10**.

The breaking of $Z(4)$ down to $Z(2)$ for sufficiently negative H_A is manifest in histograms of the Polyakov loop in the fundamental representation as a clustering of data around either the x or y axis, but not both, as shown in Figs. 13–16. Note that Fig. 14 reflects a single tunneling event. The $Z(2)$ character of this new phase is very clearly shown in Fig. 17, which shows the behavior of the real and imaginary part of the Polyakov loop versus Monte Carlo

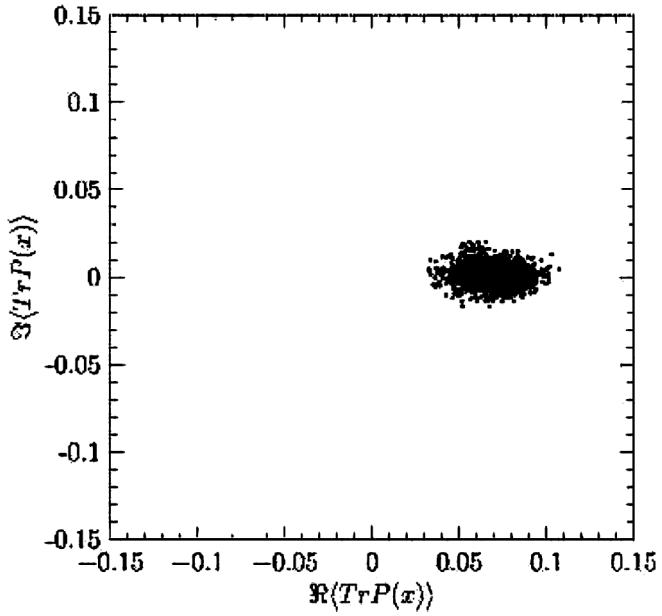

FIG. 13. $SU(4)$ Polyakov loop histogram at $\beta = 11.1$, $H_A = -0.1$.

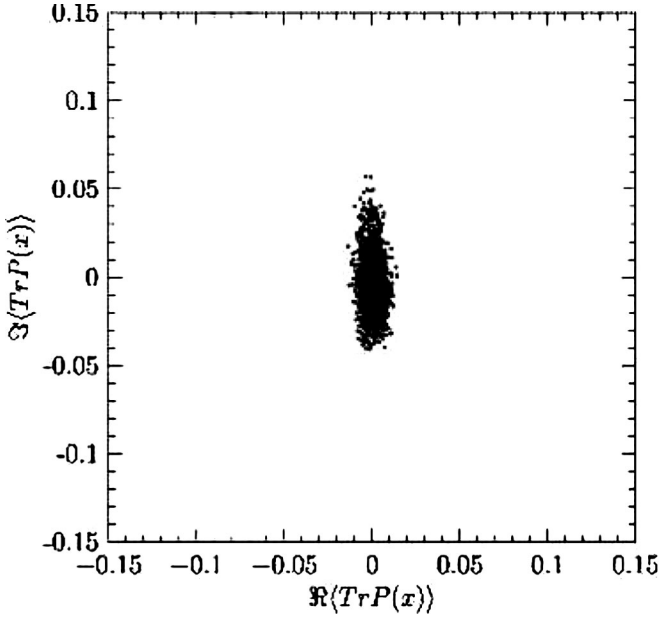

FIG. 15. $SU(4)$ Polyakov loop histogram at $\beta = 11.1$, $H_A = -0.12$.

time for one long run with 20 000 measurements and multiple tunneling events. As the figure reveals, there are significant fluctuations in either the real or the imaginary part, but not both simultaneously, characteristic of $Z(4)$ breaking to $Z(2)$. In this phase, the expectation value of $\mathrm{Tr}_F P^2$ is nonzero, being positive when the fluctuations in $\mathrm{Tr}_F P$ are along the real axis, and negative when $\mathrm{Tr}_F P$ fluctuates along the imaginary axis.

As H_A becomes more negative. the histograms show decreasing amplitude in the fluctuations of $\mathrm{Tr}_F P$. It is possible that there is a second phase transition from the $Z(2)$ phase to the confined phase as H_A becomes more negative, but we have not found direct evidence for this. As we discuss below, our simple theoretical model does not predict a second transition for this theory, at least not at high temperatures where it is valid.

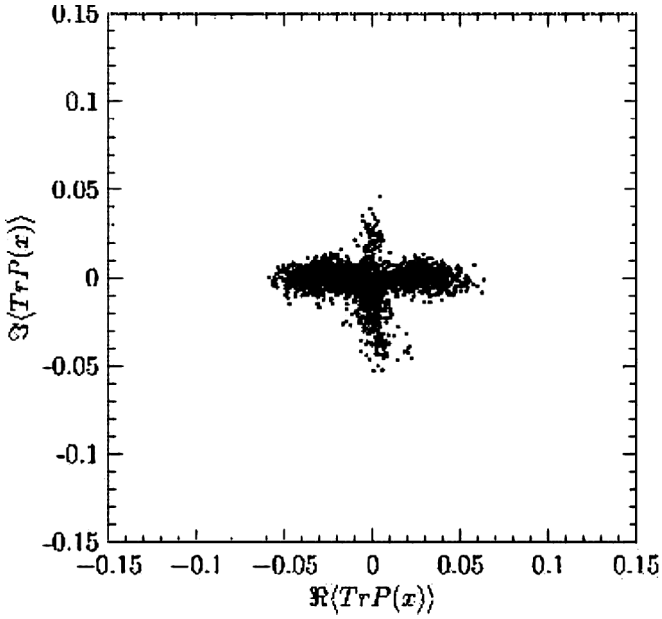

FIG. 14. $SU(4)$ Polyakov loop histogram at $\beta = 11.1$, $H_A = -0.11$.

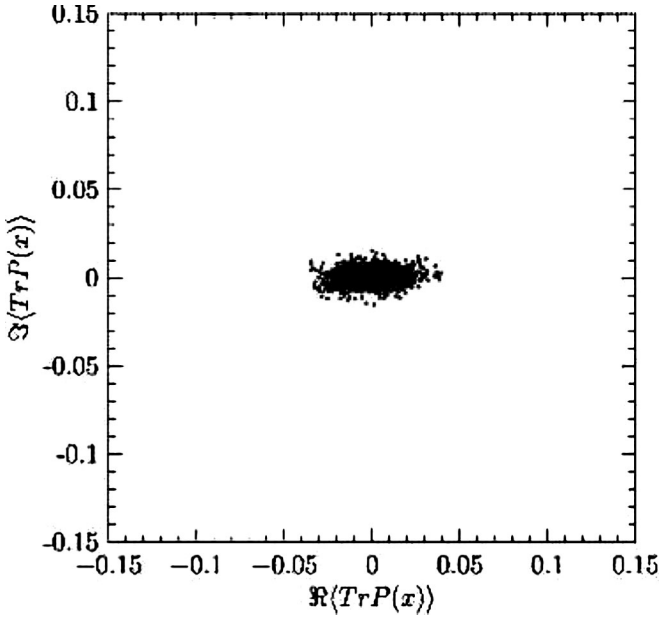

FIG. 16. $SU(4)$ Polyakov loop histogram at $\beta = 11.1$, $H_A = -0.125$.

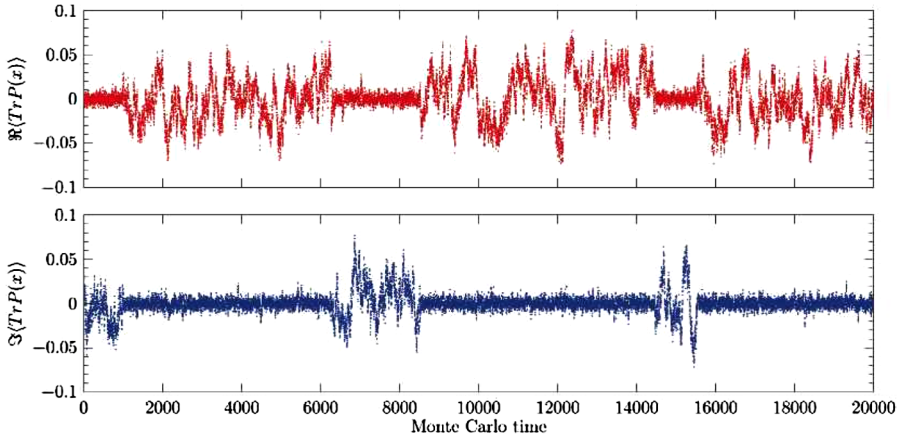

FIG. 17 (color online). Real and imaginary parts of $SU(4)$ Polyakov loop versus Monte Carlo time at $\beta = 11.1$, $H_A = -0.11$.

V. THEORY FOR $SU(4)$

We have examined within our simple theoretical model the possible occurrence of four different phases in $SU(4)$: the confined phase, which has full $Z(4)$ symmetry; the deconfined phase; a partially-confined, $Z(2)$-invariant phase; and a skewed phase similar to the skewed phase of $SU(3)$. Only the deconfined phase and the $Z(2)$ phase are predicted by our simple theoretical model.

The properties of the $Z(2)$-invariant phase may be understood by considering the one-parameter class of eigenvalues invariant under $Z(2)$; the eigenvalues in this class may be written as $\{\theta, \pi - \theta, \pi + \theta, 2\pi - \theta\}$, and the corresponding Polyakov loops have the form $\mathrm{diag}[e^{i\theta}, -e^{-i\theta}, -e^{i\theta}, e^{-i\theta}]$. The one-loop effective potential as a function of θ becomes

$$V_{\mathrm{eff}} = -\frac{\pi^2 T^4}{3} + \frac{T^4}{6\pi^2}[(\pi - 2\theta)^2(\pi + 2\theta)^2 + \pi^4 + (2\pi - 2\theta)^2(2\theta)^2] + h_A T \tag{10}$$

which has its minimum within this class at $\theta = 0$. The confined phase, which has $Z(4)$ symmetry, is realized at $\theta = \pi/4$ but is never the minimum of V_{eff}. This behavior is easy to understand: both the confined and $Z(2)$-invariant phases have the same dependence on h_A, so the stable phase is the one that minimizes the contribution of the gauge bosons. The deconfined phase does not fall into the $Z(2)$-invariant class: with all eigenvalues set to 0, the value of the effective potential in the deconfined phase is

$$V_d = -\frac{\pi^2 T^4}{3} - 15 h_A T. \tag{11}$$

There is a first-order transition between the deconfined and $Z(2)$-invariant phases at $h_A/T^3 = -\pi^2/48 \simeq -0.205\,617$. The value of $\Delta(p/T^4)$ between $h_A = 0$ and the critical point is $\pi^2/3 \simeq 3.289$. The value we obtained from simulations at $\beta = 11.0$ was 2.21 ± 0.07, where again the systematic error dominates, due to uncertainty in the location of the transition.

In order to realize the confined phase, it may be necessary to add an additional term proportional to $\mathrm{Tr}_A P^2 = \mathrm{Tr}_F P^2 \mathrm{Tr}_F P^{+2} - 1$ in order to force both $\mathrm{Tr}_F P$ and $\mathrm{Tr}_F P^2$ to zero, but this has not yet been checked in simulations. In addition to the transition line separating the deconfined phase from the $Z(2)$ phase, there must also be a line of transitions in the $\beta - H_A$ plane separating the $Z(2)$ phase from the low-temperature confined phase with $Z(4)$ symmetry. This transition could be either first or second order. We have not yet mapped out this phase boundary via simulation. It is possible that this transition line is predominantly vertical in the $\beta - H_A$ plane. As previously noted, our simple theoretical model does not include a mechanism for this transition.

VI. CONCLUSIONS

We have considerable evidence, from lattice simulation and from theory, for the existence of new phases of finite-temperature gauge theories, and for the restoration of the confined phase at high temperatures when extra, $Z(N)$-invariant, Polyakov loop terms are added to the gauge action. In $SU(3)$, a novel skewed phase was found, and in $SU(4)$, we found a phase where $Z(4)$ is spontaneously broken to $Z(2)$. In the general case of $SU(N)$, there is good reason to expect a very rich phase structure may exist.

A simple theoretical model based on perturbation theory at high temperatures has proven surprisingly accurate in predicting the observed phase structure and thermodynamics. Although successful, the model has significant shortcomings. Fluctuations in A_0 are not considered, nor is the renormalization of h_A. Most importantly, our simple model does not include in V_{eff} whatever mechanism is responsible for confinement at low temperatures when $h_A = 0$. It is therefore invalid at low temperatures. Nevertheless, theory and simulation are in reasonable agreement on a wide range of properties. Our model can also make predictions for string tensions and 't Hooft loop surface tensions, and

these predictions can be checked in lattice simulations. The introduction of h_A as an extra parameter also affects the action of calorons, topologically stable solutions of the classical field equations, and thus may offer rich possibilities for explorations in instanton physics.

The interpretation of these additional phases of finite-temperature gauge theories is, to a degree, associated with the issue of a physical implementation of a negative value for h_A. The existence of a partially confining, $Z(2)$-invariant phase in $SU(4)$ might have been expected [12], and the interpretation of the order parameters is clear. The interpretation of the skewed phase in $SU(3)$ is less certain. As in the deconfined phase, the global symmetry of the Polyakov loop is lost in the skewed phase. Our theoretical analysis indicates that, on average, two of the three Polyakov loop eigenvalues are degenerate, suggesting a possible interpretation of the skewed phase as some form of $SU(2) \times U(1)$ Higgs phase.

The issues underlying the interpretation of parameters and phases is connected with the association of finite-temperature gauge theories with universality classes of spin systems [1]. It has always been assumed implicitly that the mapping from gauge theories to spin systems is into but perhaps not onto. There are phases of $SU(N)$ and $Z(N)$ spin systems which are not easily obtainable from physical finite-temperature gauge theories. For example, the antiferromagnetic phase of a spin system can be obtained from the strong-coupling effective action of a lattice gauge theory with $g^2 < 0$ and N_t odd, a construction with no obvious continuum limit. However, phases can often be reached in different ways in the space of parameters. The skewed phase we have found in $SU(3)$ gauge theory is very similar to the anticenter phase found in $SU(3)$ spin systems by Wozar *et al.* [14]. Although the term in the spin Hamiltonian that produces the anticenter phase is associated with the **15** representation rather than the adjoint term we have used, we are confident that the two phases will prove to be related. At this time, it is simply unclear what physical principles, if any, limit the map between spin systems and gauge theories.

Changes in phase structure as the boundary conditions are varied have also been seen for fermions in the fundamental representation in $SU(3)$ [15]. For both fundamental and adjoint representation fermions with periodic boundary conditions, the basic physics is similar. At high temperatures, the gauge field contribution to the effective potential tends to maximize $\mathrm{Tr}_A P$, while the fermionic contribution tends to minimize $\mathrm{Tr}_R P$, where R is either the fundamental or adjoint representation. In both cases, it is the conflict between these two terms that gives rise to an interesting phase structure. In the case of fermions in the fundamental representation where N is odd, periodic boundary conditions give rise to phases which break charge conjugation symmetry, signaled by an imaginary part to the expectation value of $\mathrm{Tr}_F P$ [15]. These phases have a net baryonic current [16]. For adjoint fermions, charge conjugation symmetry is not broken, because a global $Z(N)$ transformation rotates $\mathrm{Tr}_F P$ to the real axis. In the case of adjoint Majorana fermions, there is no conserved fermion number current. Thus the phase structures that flow from the same fundamental physics are distinct for fermions in the fundamental and adjoint representations of $SU(3)$. As we have seen in the case of $SU(4)$, for higher values of N adjoint fermions do not necessarily behave in the same way as the case of $SU(3)$.

We believe that the ability to create new phases in a controlled way may become an important tool in understanding the properties of finite-temperature gauge theories. For example, simulations indicate that the confined phase obtained in $SU(3)$ at high T with $h_A < 0$ is connected to the conventional confined phase at low T with $h_A = 0$. The possibility of a confined phase in a region where perturbation theory is valid is by itself enormously interesting. As larger gauge groups are considered, the number of possible new phases increases. For example, in $SU(6)$, we can consider partial breaking of $Z(6)$ to either $Z(2)$ or $Z(3)$. At high temperatures, analytic calculations of both string tensions and 't Hooft loop surface tensions can be carried out in these different phases of $SU(6)$ for potential comparison with simulation [17].

[1] B. Svetitsky and L. G. Yaffe, Nucl. Phys. **B210**, 423 (1982).
[2] N. M. Davies, T. J. Hollowood, V. V. Khoze, and M. P. Mattis, Nucl. Phys. **B559**, 123 (1999).
[3] N. M. Davies, T. J. Hollowood, and V. V. Khoze, J. Math. Phys. (N.Y.) **44**, 3640 (2003).
[4] D. Diakonov, N. Gromov, V. Petrov, and S. Slizovskiy, Phys. Rev. D **70**, 036003 (2004).
[5] P. N. Meisinger and M. C. Ogilvie, Phys. Rev. D **65**, 056013 (2002).
[6] M. Di Pierro and J. M. Flynn, Proc. Sci., LAT2005 (2006) 104 [arXiv:hep-lat/0509058].
[7] P. de Forcrand and O. Jahn, arXiv:hep-lat/0503041.
[8] M. Hasenbusch and S. Necco, J. High Energy Phys. 08 (2004) 005.
[9] A. Bazavov, B. A. Berg, and U. M. Heller, Phys. Rev. D **72**, 117501 (2005).
[10] D. J. Gross, R. D. Pisarski, and L. G. Yaffe, Rev. Mod. Phys. **53**, 43 (1981).
[11] N. Weiss, Phys. Rev. D **24**, 475 (1981).

[12] P. N. Meisinger, T. R. Miller, and M. C. Ogilvie, Phys. Rev. D **65**, 034009 (2002).
[13] M. Schaden, Phys. Rev. D **71**, 105012 (2005).
[14] C. Wozar, T. Kaestner, A. Wipf, T. Heinzl, and B. Pozsgay, Phys. Rev. D **74**, 114501 (2006).
[15] T. DeGrand, R. Hoffmann, and J. Najjar, J. High Energy Phys. 01 (2008) 032.
[16] B. Lucini, A. Patella, and C. Pica, Phys. Rev. D **75**, 121701 (2007).
[17] M. C. Ogilvie, P. N. Meisinger, and J. C. Myers, Proc. Sci., LAT:213 (2007) [arXiv:0710.0649].